PROGRAMMABLE
MATERIALS

REVIEW ARTICLE

Programmable polymers with shape memory for biomedical applications

Kaojin Wang [1], Limin Man[1], Meng Zhang[2], Yong-Guang Jia[3] and X. X. Zhu [4]*

[1]School of Materials Science and Engineering, Liaocheng University, Liaocheng, China.
[2]Institute of Atomic and Molecular Physics, Sichuan University, Chengdu, China.
[3]School of Materials Science and Engineering, South China University of Technology, Guangzhou, China.
[4]Département de Chimie, Université de Montréal, Montréal, QC, Canada.

Author for correspondence: X. X. Zhu, Email: julian.zhu@umontreal.ca

Abstract

Shape memory polymers (SMPs) are a type of programmable materials capable of transforming their shapes in a pre-programmed way upon the application of an external stimulus. These materials have been tested for various potential applications particularly in the biomedical field for polymers with general and specific requirements. This review focuses on the recent advances in biomedical applications, including self-tightening sutures, pressure bandages, self-expansion stents, tissue engineering scaffolds, artificial muscles, drug delivery, and orthodontic archwires, after a brief description of the concepts, classifications, programming procedures, and material requirements of SMPs.

Contents

Introduction

Programmable materials can manifest changes in their physical properties (i.e., shape, density, mechanical properties, and optical properties) when an external stimulus is applied according to a certain initial design and pre-programming. Shape memory polymers (SMPs) may change their shapes

in a pre-programmed way upon exposure to certain external stimuli and can be classified as a family of programmable materials. These external stimuli may be changes in temperature (Li et al. (2018); Wei et al. (2018)), light (Zhang et al., 2014; Wang and Zhu, 2018; Wu et al., 2019; Liang et al., 2021), electrical field (Lu et al., 2014; Wang et al., 2015; Gong et al., 2016; Qian et al., 2017), magnetic field (Cai et al., 2013; Razzaq et al., 2013, 2014; Zhang et al., 2015; Gu et al., 2016; Du et al., 2018; Wang et al., 2018), pH (Li et al., 2015; Le et al., 2017; Wu et al., 2022), and solvent (Xiao et al., 2015; Hou et al., 2018; Li et al., 2020). Conventional SMPs cannot reverse spontaneously to their temporary shapes under a stimulus after returning to their permanent shapes unless they are reprogrammed by applying an external force, which is classified as one-way SMPs (Wang et al., 2020). According to the number of memorised temporary shapes, one-way SMPs can be classified as dual, triple, and multiple (quadruple, quintuple, etc.) SMPs, which can memorise one, two, and three or more temporary shapes, respectively (Wang et al., 2015, 2017). Two-way SMPs may transform reversibly between two different shapes when they are exposed to two intrinsically inverse stimuli, such as heating and cooling (Wang et al., 2017, 2019, 2020).

SMPs have found applications in various fields, including biomedicine (Wang et al., 2022), smart textiles (Hu et al., 2012), actuators (Liu et al., 2021; Xu et al., 2021), aerospace (Xia et al., 2020), and sensors (Leo et al., 2018). Biocompatibility and nontoxicity are among the most desired properties for biomedical applications (Cao et al., 2021; Tian et al., 2021). In addition, actuation temperature close to body temperature (Ahmad et al., 2011), satisfactory mechanical properties, and facile processability are also essential. Their applications are largely determined by their properties and specific functions. For instance, a device can be implanted in a compressed shape through key-hole incisions and expand to its original shape in the body. The actuation in the body may be triggered by applying different stimuli, such as heating, light, and magnetic fields. Thus, a proper range of external stimuli is crucial for the safety of patients. For example, irreversible tissue damage may occur when the temperature is increased to 42°C (Li et al., 2020). Indirect heating is used more often than direct heating due to its convenience of actuating SMPs in vivo. Light and magnetic fields are the most common stimuli of indirect heating. Infrared (IR) light instead of ultraviolet (UV) light is usually used to heat an SMP since it has good photothermal effect and large penetration depth, and it is regarded as harmless to the human body. The radio-frequency range (roughly from 1 kHz to 1 MHz) of the magnetic field is regarded as safe for the human body and has a large penetration depth to access organs or tissues in the body (Bañobre-López et al., 2013). In addition, the design and programming of the shapes and functions are important for their successful application. The use of SMPs in the biomedical field has been tested as surgical sutures, pressure bandages, drug delivery carriers, self-expansion stents, tissue engineering scaffolds, artificial muscles, drug delivery carriers, and orthodontics. The application aspect of these materials is the focus of the current review.

Programming procedures of SMPs

One-way SMPs include dual, triple, and multiple SMPs which involve the switching between two, three, or more shapes, the permanent shape being counted. Dual SMP is the simplest one relying only on one thermal transition. Most of the polymers may show a dual-shape memory effect because they show at least one thermal transition. These polymers include polyesters, polyurethanes, polyethers, polyelectrolytes, and polyimide. Polyesters usually show biodegradability, which includes poly(lactic acid) (PLA), poly(ε-caprolactone) (PCL), and poly(p-dioxanone). Poly(ethylene glycol) is the most reported SMP for polyethers. They are most commonly reported for their potential use in biomedicine. The programming procedures of thermally induced dual SMPs are concisely presented here for a better understanding of the shape changes, while some descriptions can also be found in several review papers (Lendlein and Kelch, 2002; Xie, 2011; Zhao et al., 2015; Wang et al., 2019; Delaey et al., 2020; Scalet, 2020). The SMP is first stretched at a temperature higher than its transition temperature (T_{trans}), which may be a glass transition temperature (T_g), melting temperature (T_m), or clearing temperature (T_{cl}). The changes in the conformations of the activated polymer are characterised by a reduced entropy.

The sample is then cooled below its T_{trans} to trap the conformation of the polymer chains, fixing the temporary shape of the polymer. The corresponding elastic energy of the reduced entropy is thus stored. After unloading the external force, the temporary shape is fixed and may be kept for a long time at this temperature. This can be characterised by the fixity ratio R_f:

$$R_f = \frac{\varepsilon(N)}{\varepsilon_{load}(N)} \times 100\%, \tag{1}$$

where ε_{load} is the maximum strain before forgoing the external load, ε represents the strain after cooling and removing the external force, and N indicates the number of cycles in the shape memory test. When the SMP is heated above its T_{trans} again, the movement of polymer chains is reactivated, producing a shrinkage force. Thus, the SMP returns to its permanent shape. This can be characterised by the recovery ratio R_r:

$$R_r = \frac{\varepsilon(N) - \varepsilon_{rec}(N)}{\varepsilon(N) - \varepsilon_{rec}(N-1)} \times 100\%, \tag{2}$$

where ε_{rec} is the strain after recovery.

Triple and multiple (quadruple, quintuple, etc.) SMPs may involve the memory of three and four or more shapes (counting the permanent shape), which may depend on two or more T_{trans}s. One broad T_{trans} may also endow polymers with triple and multiple shape memory effects (SMEs). For example, triple SMPs need one extra deformation, fixation, and recovery programming procedure needs to be operated on the material, while for quadruple SMPs two such additional programming states are needed for deformation, fixation, and recovery. The programming procedures for other multiple SMPs can be inferred to likewise (Wang et al., 2019). Unlike one-way SMPs, two-way SMPs depend on the phase transition of polymer crystals or liquid crystals upon heating and cooling, leading to melting-induced contraction and crystallisation-induced elongation. Since the two-way SMPs may or may not require the application of an external force, they are further divided into 2W-SMPs under stress and stress-free conditions. Their programming procedures have also been elaborated previously (Wang et al., 2019).

Material requirements for biomedical applications

For practical biomedical applications, SMPs need to meet general and specific requirements (Delaey et al., 2020). The former ones include nontoxicity, biocompatibility, and easy processability, while the latter involves mechanical properties, biodegradability, antibacterial property, porosity, and stability.

Nontoxicity is the first general requirement for the usage of SMPs in biomedical applications. The materials are required to be non-teratogenic, non-allergic, non-mutagenic, non-mutagenic, non-carcinogenic, non-pathogenic, and non-stimulating. Biocompatibility is the second general requirement, which means that the implanted biomaterials would not induce immune response and inflammatory response. The blood compatibility should be insured for SMPs implanted into our body and exposed to blood. One typical example is self-expansion stent acting as an intravascular stent for which neither hemolysis nor thrombosis should occur on the polymer surface. Easy processability is also very important, which determines the cost and practical use. The structure of some biomedical devices could be constructed by advanced processing technology. For example, high porosity scaffolds may be obtained by using 3D printing so that new bone tissue is able to infiltrate the porous structure.

Specific requirements are related to the practical applications. Different applications may need different or even opposing material properties. The mechanical properties of the materials are the ability to resist mechanical forces, which need to be matched in specific applications. For example, the actuation stress of artificial muscles made by biomaterials should be higher than that of human skeletal muscle (0.35 MPa) (Wang et al., 2018). Another example is the stress relaxation of bandages which may cause pressure drop and weaken the intended application. Hence, low-pressure relaxation is necessary for bandages. Moreover, mechanical resistance is also essential for certain applications. For instance, self-expansion stents need to be left in the body permanently, so they must exhibit

adequate mechanical resistance to hold open passages. Applications such as pressure bandages and orthodontic archwires also require good mechanical properties to be maintained during the time of usage. Good mechanical resistance of SMPs can be achieved by introducing chemical cross-linking in the structure and by inclusion of non-degradable components. Biodegradability may be regarded as the opposing material property of mechanical resistance, which is desirable in certain biomedical applications. Surgical sutures used to close wound tissues need to be removed after clinical healing, resulting in secondary damage and leaving scars. In this case, biodegradable sutures are highly desirable so that they can be absorbed or degraded after a certain duration. Another example is tissue engineering scaffolds which need to be degraded or absorbed and replaced by new tissue gradually. Biodegradable SMPs usually originate from renewable or petroleum resources. The former can be made of natural compounds, such as bile acids (Gautrot and Zhu, 2009), plant oils (Mu et al., 2020), and cinnamate group (Wang et al., 2015), while the latter can be made of glycolide, lactide, ε-caprolactone, and p-dioxanone. The introduction of antibacterial molecules into SMPs may render the materials with antibacterial properties preventing the occurrence of infections, which is especially important for materials implanted in the human body.

Biomedical applications

Self-tightening sutures

Surgical sutures are used to close wounds to skin or other tissues and help in holding them together. The secondary damage may be usually caused by wound suture and suture removal. Bioabsorbable sutures have been used in recent years. However, the surrounding tissue necrosis may still be caused if the force of suture is relatively high. The wound may be sutured loosely if the force is relatively low, leaving obvious scars. The surgical sutures made of SMPs may solve such problems since SMPs may provide a steady and uniform recovery force.

Lendlein and Langer (2002) first reported self-tightening sutures made by biodegradable multiblock copolymers poly(caprolactone-dioxanone), in which oligo(ε-caprolactone) acted as the switching segments and oligo(p-dioxanone) served as the hard segments. Both oligomers were synthesised by using ring-opening polymerisation of cyclic diesters or lactones. The authors programmed the polymer fibres by stretching to 200% and then fixed their shapes with fixity ratios up to 99.5%. The wound was then loosely sutured by the polymer thread through a surgical needle. When the temperature rose to 41°C, the suture contracted automatically, and the wound gap was closed. Since then, more self-tightening sutures made of various polymers have been reported.

The device of self-tightening knot can serve as a demonstration of self-tightening suture. For example, we have designed and made shape memory polyesters based on bile acid derivatives. The loosely knot of the stretched sample was tighten automatically by raising the temperature (Gautrot and Zhu, 2009). Turng and colleagues reported that thermoplastic polyurethane (PU)/PCL blends showed thermo-induced shape memory effect and self-knot capability (Jing et al., 2016). Self-tightening knots triggered by other stimuli have also been reported. Toncheva et al. (2018) synthesised a photothermal filler by grafting plasmonic silver nanoparticles onto cellulose nanocrystals. A low loading (1 wt%) of the resultant filler was then introduced into PCL-based networks, producing remote actuated SMPs upon infrared light irradiation. A self-tightening knot was also demonstrated when shone by an IR lamp for 30 s.

A surgical site infection caused by bacteria occurs often after surgery. Therefore, the sutures with antibacterial activity have been developed by introducing antibacterial compounds into SMPs. For example, Tian and coworkers fabricated surgical sutures by incorporating antibacterial berberine hydrochloride (BCH) into the solution of shape memory polyurethane (SMPU) with a T_{trans} slightly higher than body temperature and following one-step wet spinning. The authors first sutured the wound loosely by using the elongated fibre which was tightened automatically after raising the temperature (Figure 1a). Mouse skin suture-wound model was tested for evaluating wound healing and antimicrobial
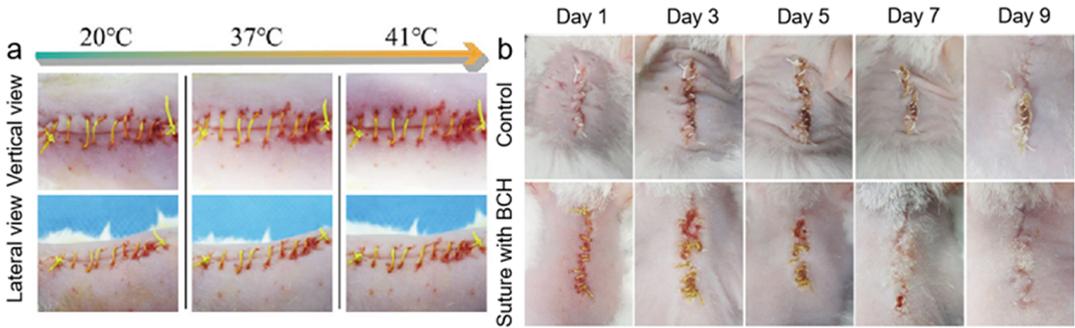
Figure 1. *(a) Self-tightening ability of SMP suture containing BCH at various temperatures as indicated, and (b) the wound healing process after bacterial inoculation. Adapted with permission from Zhou et al. (2019). Copyright from Frontiers.*

activity. As shown in Figure 1b, the wound was inoculated with *S. aureus* and then sutured by using the polymer fibre without or with BCH. After 9 days, scab and necrotic tissue still remained for the wounds sutured with pure SMP fibre, while the wounds sutured with BCH-based fibre reached clinical healing (Zhou et al., 2019). The same group made another antibacterial self-tightening suture by incorporating polyhexamethylene biguanide hydrochloride instead of BCH into SMPU. Similar results were obtained (Chen et al., 2020). Maiti and coworkers synthesised SMPU nanohybrid in the presence of organically modified nanoclay and then used it for suturing the incision of a rat loosely with a 2 mm gap. The gap was closed in 6 s after triggering the shape recovery of the suture by heating it to ~37°C. They found that clinical healing of the incision was completed in 7 days with no scar formed (Biswas et al., 2018).

Pressure bandages

The conventional bandages made of gauze or cotton wool are usually used to treat wounds, which can supply pressure to control fluid retention and reduce the swelling of the tissue. Nevertheless, conventional pressure bandages cannot supply sustained compression to the joint due to the irregular shape and inevitable movement of the joint. Moreover, fibres are usually left in wounds during bandage removal. A painful rash may also occur due to prolonged treatment. Pressure bandages made by SMPs may address these problems due to their large contraction upon external stimuli, biocompatibility, easy processability, and even bioabsorbability.

Ahmad et al. reported for the first time the use of SMPs for the design of pressure bandages. Two kinds of bandages were designed and prepared by attaching pre-stretched strips of thermo-induced SMPs with a low T_{trans} of ~50°C on the fabric. These pre-stretched strips consist of either a fixed strain with varying lengths or a fixed length with varying strains (Figure 2a,b). Around the model leg, the SMP strips partially shrank to their original lengths by using a heat gun or a hot towel, producing a coaxial force acting inwards by pre-defined shrinking force and pressure distribution for venous leg treatment (Figure 2c,d). A typical pressure required for the leg ulcer treatment at ankle was 40 mmHg, and it decreased to 15 mmHg at the upper part of the leg (Figure 2e) (Ahmad et al., 2012). Kabir and colleagues synthesised chemically cross-linked hydrogels using *N,N*-dimethyl acrylamide and stearyl acrylate. The hydrogels exhibited SMEs by heating to 42.5°C above their T_{trans} values. The potential application as a medical bandage for broken bones was also demonstrated (Figure 3). The hydrogel was first deformed into elongated, twisted, and coiling shapes (Figure 3b–d) at a temperature higher than its T_{trans}. The deformed hydrogel was then coiled on broken bones and cooled below its T_{trans} for fixation (Figure 3e). The bandage can be removed by simple heating without the need of scissors or expert nurses (Hasnat Kabir et al., 2014).
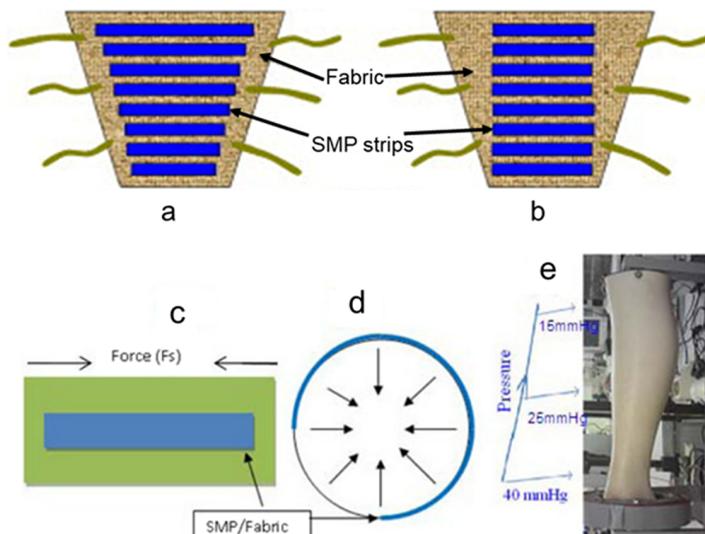
Figure 2. *(a,b) Schematic illustration of two kinds of SMP/fabric artificial bandages, (c) an artificial bandage made by an SMP strip fixed on a fabric, (d) the produced co-axial force after wrapping, and (e) the required pressure for the leg ulcer treatment. Reproduced with permission from Ahmad et al. (2012). Copyright from Taylor & Francis Online.*
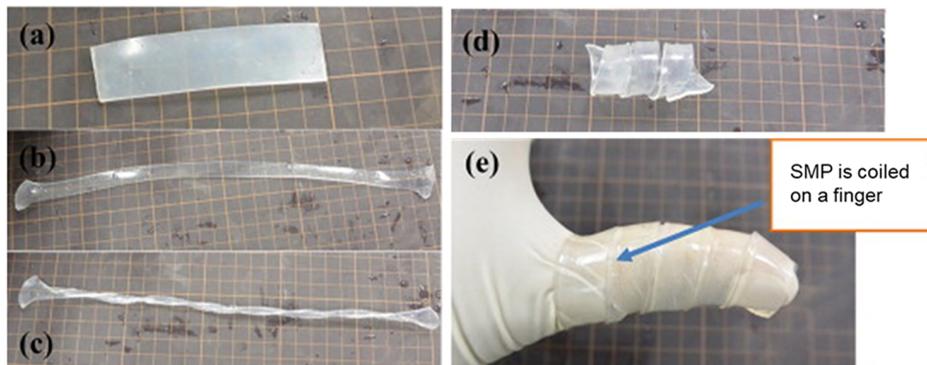

Figure 3. *Photographs showing shape memory gel deformation and application. (a) Original shape, (b) elongated shape, (c) twisted shape, (d) coiling shape, and (e) coiled shape as a bandage. Reproduced with permission from Hasnat Kabir et al. (2014). Copyright from Elsevier.*

Besides SMP sheets, textiles made of shape memory filaments can also be designed as smart bandages. Hu and coworkers developed blend yarns made of SMPU and nylon filaments that can yield an optimal shape and compression pressure. The bandage may control or manage the pressure in a wrapped position. Heating this product can produce extra pressure (up to 50%) due to the contraction (Kumar et al., 2016; Narayana et al., 2018). Other stimuli can also trigger the shrinkage of SMP bandage. For example, Jiang and coworkers reported that a zwitterionic SMP was synthesised by copolymerizing sulfobetaine methacrylate, 2,3-dihydroxypropyl methacrylate, and a cross-linking agent of boric acid. Such an SMP exhibited both thermo- and moisture-responsive shape memory behaviours, and may be applied as a smart bandage due to its contraction capability from extended temporary shape to the original shape induced by hot vapour (Figure 4; Li et al., 2018).
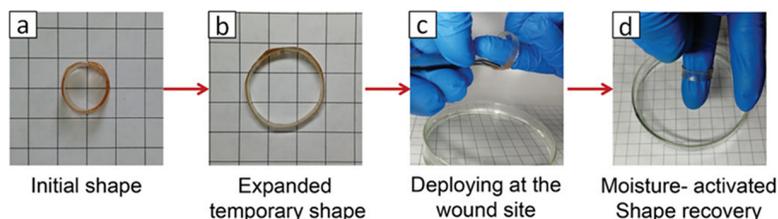
Figure 4. The pre-programming process and the potential application as smart bandage of a zwitterionic SMP. Reprinted from Li et al. (2018) with permission. Copyright from Wiley-VCH.

Self-expansion stents

A self-expansion stent is used to hold open passages in our body and leave there permanently. Over the past decades, metallic stents have been used to treat narrowed coronary arteries. However, many long-term side effects, such as thrombus and intimal hyperplasia, may be caused by the metallic stents. Restenosis rates of 20 to 40% in patients also limit their further development (Essandoh et al., 2017). Biodegradable polymeric stents with self-expansion ability may be desirable products to replace metallic ones. They can open passages in the short term and avoid thrombus and restenosis. SMPs may be used to design such a stent due to their shape-changeable capability.

The first polymeric stent implanted in human coronary artery is the Igaki-Tamai stent made of biodegradable PLA. However, the self-expansion behaviour has to be realised by a heated balloon, which may cause damage to the vessel (Tamai et al., 2000). The concept of an SMP stent for drug delivery application was then proposed by Wache et al. (2003). After that, various self-expansion stents made of SMPs have been reported. Bellin et al. (2006) synthesised chemically cross-linked polymer networks containing PCL and poly(ethylene glycol) (PEG) segments with triple shape memory effect. Their design of a removable stent with a compressed shape first expanded to a round shape when heated to 40°C, and then shrank to a shape with a smaller diameter at 60°C for easy extraction.

The stents with helical structure are reported commonly due to their easy processing without special tools. The processing procedures of the helical stents may be generally summarised as follows. A polymer strip is wrapped around a mandrel and heated above its T_{trans} for heat shaping. The stent is then wound onto a shaft of smaller diameter and cooled to room temperature for shape fixation. It is stored at room temperature prior to implantation. The first reported example is a bilayered biodegradable stent prepared from PLA and poly(glycolic acid), which can self-expand at 37°C (Venkatraman et al., 2006). Afterwards, Li and coworkers used a similar processing method to prepare SMP stents from block copolymers consisting of hyperbranched three-arm PCL and poly[(R)-3-hydroxybutyrate-co-(R)-3-hydroxyvalerate], which could self-expand nearly completely at 37°C within only 25 s (Xue et al., 2010). Similar self-expansion stents were also reported by other researchers using similar processing methods (Yang et al., 2013; Biswas et al., 2018; Zeng et al., 2020). Besides thermo-responsive SMP stents, water-responsive SMP stents made of the blend film of glycerol, PEG, and chitosan, were also reported. The helical-shaped stent self-expanded upon hydration. The stent was implanted into the rabbit's abdominal aorta, which was found to be intact with no thrombus in the vessel (Chen et al., 2007). However, self-expandable stents with complicated structure cannot be made by this easy processing method, limiting their development.

Three-dimensional (3D) printing has seen rapid development in recent years, providing a new processing technique for the preparation of stents with complex structure. Jia et al. (2018) fabricated a biodegradable vascular stent using SMP of amorphous PLA with a T_g of 58°C through 3D printing. The printed stent has a hexagon nested structure and thus can be compressed at 70°C for easy implantation. The compressed stent (temporary shape) can be well kept at room temperature with an excellent shape fixity (over 99%). After implantation, the stent could self-expand to its original shape by heating to 70°C. The problem here is that the trigger temperature is much higher than the body temperature.
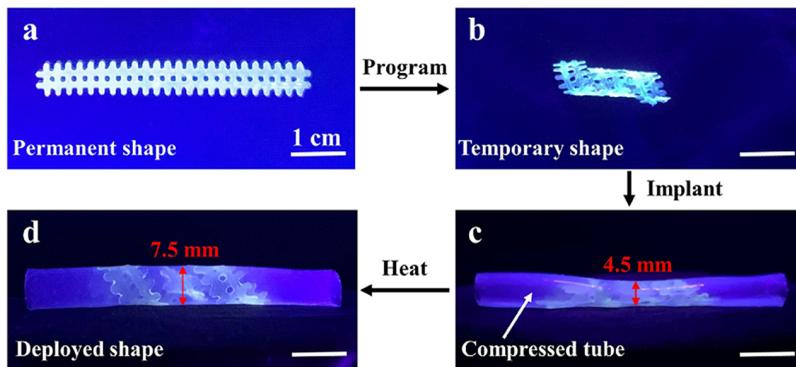
Figure 5. *The programming and self-expansion process of an SMP stent in a compressed silicone tube. Reprinted from Zhang et al. (2021) with permission. Copyright from Elsevier Ltd.*

This problem has been addressed by other researchers. Lin and coworkers printed mesh stent from poly(glycerol dodecanoate acrylate) with a T_{trans} ranging from 20 to 37°C. The stent was implanted in a compressed silicone tube and may deploy after heating above its T_{trans}, expanding the diameter of silicone tube from 4.5 to 7.5 mm (Figure 5; Zhang et al., 2021). Leng and colleagues fabricated two types of shape memory stents with negative Poisson's ratio structure by 3D printing. The structure was optimised by using the genetic algorithm. When tested in vitro in the simulated body fluid, it was found that the narrow blood vessel could be expanded within 5 s (Lin et al., 2020). Since indirect heating cannot be conveniently realised in the human body, other stimuli-responsive self-expansion stents have been developed. Leng and coworkers also printed PLA/Fe$_3$O$_4$ composite tracheal stents with various structures. Such stents could expand completely in a magnetic field within 40 s. The stent also showed IR light-responsive self-expansion behaviour due to the high absorption rate of IR (Zhang et al., 2021).

Tissue engineering scaffolds

SMPs have also been used to design bone tissue engineering scaffolds. Three factors, including seed cells, cell growth factors, and the materials of scaffolds, may affect tissue construction and regeneration. Thus, tissue engineering scaffolds, which may offer space for cell growth, proliferation, and differentiation, play a critical role in the treatment of bone defects. The shape memory scaffold can be implanted in a compressed form (the temporary shape) and recovered to a swollen form (the original shape) when exposed to body temperature.

The scaffolds with porous structure are the most often reported (Liu et al., 2014; Senatov et al., 2016; Yu et al., 2018; Zhang et al., 2018; Beltran et al., 2021; Pfau et al., 2021; Wang et al., 2021; Zhao et al., 2021), since the inter-connected porous structure leads to a large surface area, accelerating cell attachment and growth, leading to the effective construction and regeneration of bone tissue. The preparation methods of porous polymers include templating method and electro-spinning. Zhou and coworkers developed a porous PCL/hydroxyapatite nanocomposite scaffold using sugar as the template. Bone morphogenetic protein-2 (BMP-2) and calcium alginate were then loaded into a porous scaffold. The BMP-2 loaded scaffold implanted in the rabbit mandibular defect was found to improve bone defect repair (Liu et al., 2014). Good shape recovery was observed from compressed shape to an expanded porous structure when exposed to body temperature. NaCl particles could also be used as the template to prepare porous scaffolds. Yu et al. (2018) fabricated porous SMPU/hydroxyapatite nanocomposite scaffolds using various NaCl particles as the template. The compression recovery ratio of the scaffold is higher than 99%. It was also found that the cell proliferation capability was increased with increasing apertures. Electro-spinning technique was also used to fabricate porous scaffolds for bone tissue engineering. For example, Zhang and coworkers prepared fibrous scaffolds
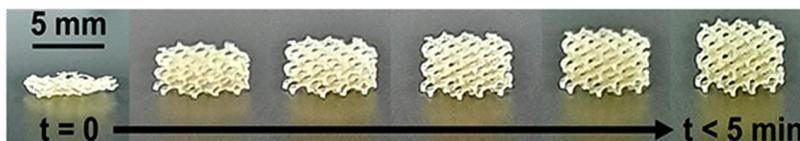
Figure 6. *The recovery process of a porous scaffold. Reprinted from Le Fer and Becker (2020) with permission. Copyright from American Chemical Society.*

of biodegradable poly(D,L-lactide-*co*-trimethylene carbonate) by electro-spinning. It was shown that the shape memory scaffolds could support osteoblast attachment, proliferation, and bone formation (Bao et al., 2014). Solution-casting method can also be used to fabricate tissue scaffolds. Filion et al. (2011) developed biodegradable PLA/polyhedral oligomeric silsesquioxane (POSS) nanocomposites via solution-casting, which can be used as self-fitting tissue scaffolds and implants. After subcutaneous implantation in rats, the scaffolds showed a mild foreign body type immune response.

Compared with conventional processing methods of porous polymers, the 3D printing technique was used to fabricate homogeneous and accurate porous structure. Becker and colleagues made high-porosity gyroid scaffolds from starred poly(propylene fumarate) by 3D printing. The bone regeneration was evaluated by using a rat as a critical-sized cranial defect model. After 4 weeks of implantation, more new bone was found in the defect of the scaffold of higher molecular weight relative to that of lower molecular weight. No noticeable evidence of immune response was found after implantation (Nettleton et al., 2019). Subsequently, the compressed scaffold showed 100% of shape recovery at 40°C in 5 min (Figure 6). The authors performed accelerated degradation tests, which showed the resorbability of the porous scaffolds (Le Fer and Becker, 2020). Recently, Langford et al. (2021) reported an interesting structural design of shape memory scaffolds with various origami structures from PLA filament by 3D printing. The scaffolds with tubular herringbone tessellation origami structure exhibited good shape deformation and shape recovery ratio of 96%.

Artificial muscles

Artificial muscles are actuators that may mimic natural muscles and generate deformations, such as elongation, contraction, and rotation, when they are exposed to an external stimulus, including temperature change, light, electric current, and humidity. Many artificial muscles made of different materials have been investigated. Compared with other materials, polymer-based artificial muscles show excellent properties, such as large deformability, light weight, flexibility, and low cost. Recently, artificial muscles based on two-way SMPs have attracted much attention due to their distinguished programmability, reversibility, and stimulus-responsive capability.

Temperature change is the most often reported trigger for artificial muscles made of SMPs (Yang et al., 2016; Yahara et al., 2019; Du et al., 2020). Fan and Li (2017) processed chemically cross-linked poly(ethylene-vinyl acetate) into fibres by a solid solution approach and fabricated artificial muscles *via* twist insertion in the precursor fibres. The resultant muscle exhibited contraction upon heating to 67°C and expansion upon cooling to 20°C with a large deformation of 68%. Light is also another common stimulus. Polydopamine nanospheres can be incorporated into two-way SMPs made of cross-linked PCL-poly(ω-pentadecalactone) PPDL network. The composite material can lift a weight upon cooling and release it under light irradiation (Figure 7). The actuated stress is around 1.1 MPa which is much larger than the stress yielded by most mammalian skeletal muscle (Wang and Zhu, 2018). Multi-stimuli responsive artificial muscles have also been investigated as shown by the artificial muscles made of cross-linked multiblock PCL-PEG PUs. The energy density of the sample was up to 717.8 kJ/m^3 which is ca. 18-fold larger than that of human skeletal muscles. The maximum reversible strain triggered by heating and cooling is about 25.7%. After incorporating Fe$_3$O$_4$ nanoparticles into the polymers,
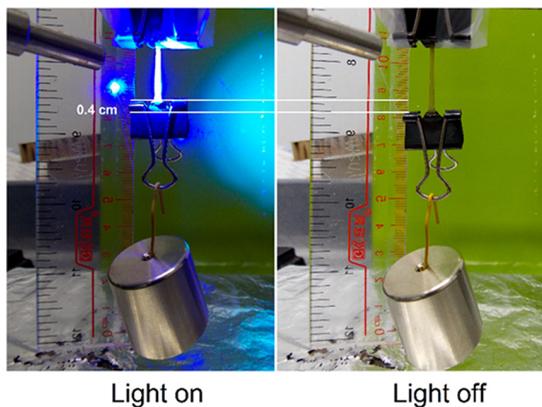
Figure 7. *The reversible lifting and releasing action realised by light actuation. Reprinted with permission from Wang and Zhu (2018). Copyright from American Chemical Society.*

contraction, reversible bending, and complex programmable deformation were realised under near-infrared laser irradiation (Zheng et al., 2021).

Drug delivery systems

Drug delivery is an active pharmaceutical research field, especially the subjects of targeted delivery and accurate control of release rate. SMPs may be useful in this area since they can store and deliver pharmaceutical compounds to the nidus in a temporary shape and release them after regaining their permanent shape when exposed to a stimulus, temperature being the most common (Melocchi et al., 2019; Inverardi et al., 2021). Melocchi et al. (2019) used the slow dissolution of the plasticized poly(vinyl alcohol) (PVA) by glycerol in water for drug delivery. The spiral shape of the PVA was embedded into capsules for the design of a potential gastric device (Figure 8). Such a device may be easily administered orally and expand to its original shape in hydrochloric solution at 37°C. Ultrasound has also been used as a stimulus to trigger drug release. Xia and coworkers prepared a series of cross-linked poly(methyl methacrylate-*co*-butyl acrylate) copolymers by changing the feeding ratios. Copper sulphate (5 wt%) was then loaded in a copolymer with a T_g of around 47°C. The shape of the composite was fixed by high-intensity focused ultrasound (HIFU) and exhibited switchable drug release when the HIFU was turned on/off. The release process may be adjusted by changing HIFU intensity and duration (Li et al., 2012). The same group also tested a PCL-based PU system (Han et al., 2013). Zhou and colleagues synthesised a pH-responsive SMP by the introduction of pyridine rings into PU backbone. They found that the formation of hydrogen bonds in neutral or alkaline environments led to the pH responsiveness which could also be broken under acidic conditions owing to the protonation of pyridine ring. Thus, drugs loaded in polymers could be released at a certain rate by the switching effect. The disruption of hydrogen bond led to the swelling of the polymer, favouring drug release, while the formation of hydrogen bond caused deswelling, suppressing drug release (Chen et al., 2014).

Orthodontic archwires

In orthodontics, the most used archwire is stainless steel or nickel-titanium alloy due to their superior mechanical properties, rigidity, durability, and antifatigue. Shape memory alloys with wire shapes have been widely used. However, metal corrosion may cause problems such as allergy, toxicity, and tooth staining, in addition to the poor aesthetics caused by the metallic colour. Attempts were made to use SMPs in orthodontics since they are easy to install, and have advantages such as adjustable shape, transparency, processability, comfortability, sustainable contraction force, and large deformation.
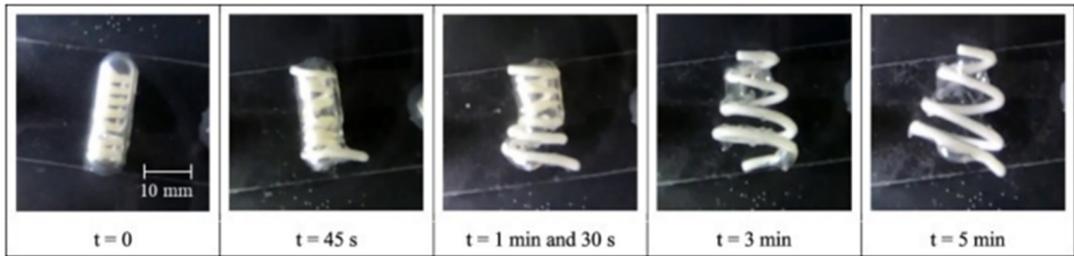
Figure 8. *Shape recovery of a temporary supercoiled shape inserted into capsule at 37°C. Reprinted from Melocchi et al. (2019) with permission. Copyright from Elsevier Ltd.*

Nakasima et al. (1991) first reported the use of thermo-responsive SMP as orthodontic archwire. The SMP archwires could supply sufficient contraction force and were more aesthetically pleasing than metallic ones. Since then, various orthodontic archwires made of SMPs were reported (Jung and Cho, 2010; Liu et al., 2017, 2018). For instance, Liu et al. (2017) used SMPU as orthodontic archwire on a wax model for a tooth-moving simulation. They found that the archwire of a 0.5 mm diameter provides restoring force in a range of 0.59 ~ 1.18 N, which meets the requirement of tooth movement (0.49–2.94 N). However, this restoring force is lower than that yielded from metallic wire. After incorporating 30 wt% short glass fibres into SMPU, the recovery force of the archwire was enhanced by 96%. For a tooth-moving simulation performed on identical typodont models, the dentition aligning time was decreased by 50% (Liu et al., 2018).

To realise the clinical application of SMP archwire, simulation experiments have been carried out. Elshazly et al. (2021) used SMP aligners to correct movement of an upper central incisor using a custom-made aligned typodont model. They found that the total correction efficiency of the used SMP aligner was up to 93%.

Conclusions and perspectives

SMPs are one type of programmable materials that have great potential in many fields, especially in biomedicine as presented in this review. Biocompatibility and nontoxicity are the most important general characteristics of such polymers, while the specific requirements are determined by their functions. Although temperature change is still the most used stimulus, indirect heating and other stimuli, such as light, electric current, magnetic field, and ultrasound, may serve more conveniently in the human body. For example, the self-expansion stents may be triggered using an electric current or a magnetic field leading to indirect heating.

Most of the biomedical applications are still at the concept stage. More efforts are needed in the technology development for commercialization. There have been promising examples such as the clinical use of self-expansion stents in the treatment of vascular and laryngeal stenosis. The work on self-tightening sutures with antibacterial properties should lead to their use in the cure of surgical wounds. The research progress in programmable materials shall undoubtedly lead to more rapid development of SMP products for use in biomedical and other fields.

References

Ahmad M, **Luo J** and **Miraftab M** (2012) Feasibility study of polyurethane shape-memory polymer actuators for pressure bandage application. *Science and Technology of Advanced Materials* **13**, 015006.

Ahmad M, **Luo J**, **Xu B**, **Purnawali H**, **King PJ**, **Chalker PR**, **Fu Y**, **Huang W** and **Miraftab M** (2011) Synthesis and characterization of polyurethane-based shape-memory polymers for tailored T_g around body temperature for medical applications. *Macromolecular Chemistry and Physics* **212**, 592–602.

Bañobre-López M, **Teijeiro A** and **Rivas J** (2013) Magnetic nanoparticle-based hyperthermia for cancer treatment. *Reports of Practical Oncology and Radiotherapy* **18**, 397–400.

Bao M, **Lou X**, **Zhou Q**, **Dong W**, **Yuan H** and **Zhang Y** (2014) Electrospun biomimetic fibrous scaffold from shape memory polymer of PDLLA-*co*-TMC for bone tissue engineering. *ACS Applied Materials & Interfaces* **6**, 2611–2621.

Bellin I, **Kelch S**, **Langer R** and **Lendlein A** (2006) Polymeric triple-shape materials. *Proceedings of the National Academy of Sciences* **103**, 18043–18047.

Beltran FO, **Houk CJ** and **Grunlan MA** (2021) Bioactive siloxane-containing shape-memory polymer (SMP) scaffolds with tunable degradation rates. *ACS Biomaterials Science & Engineering* **7**, 1631–1639.

Biswas A, **Singh AP**, **Rana D**, **Aswal VK** and **Maiti P** (2018) Biodegradable toughened nanohybrid shape memory polymer for smart biomedical applications. *Nanoscale* **10**, 9917–9934.

Cai Y, **Jiang JS**, **Liu ZW**, **Zeng Y** and **Zhang WG** (2013) Magnetically-sensitive shape memory polyurethane composites crosslinked with multi-walled carbon nanotubes. *Composites Part A: Applied Science and Manufacturing* **53**, 16–23.

Cao S, **Shao J**, **Abdelmohsen LKEA** and **Hest JCM** (2021) Amphiphilic AIEgen-polymer aggregates: Design, self-assembly and biomedical applications. *Aggregate* **3**, e128.

Chen H, **Li Y**, **Liu Y**, **Gong T**, **Wang L** and **Zhou S** (2014) Highly pH-sensitive polyurethane exhibiting shape memory and drug release. *Polymer Chemsitry* **5**, 5168–5174.

Chen X, **Tan P**, **Wen Y**, **Zhou W**, **Cen, Y**, **You C** and **Tian M** (2020) Facile scalable one-step wet-spinning of surgical sutures with shape memory function and antibacterial activity for wound healing. *Chinese Chemical Letters* **31**, 1499–1503.

Chen MC, **Tsai HW**, **Chang Y**, **Lai WY**, **Mi FL**, **Liu CT** and **Sung HW** (2007) Rapidly self-expandable polymeric stents with a shape-memory property. *Biomacromolecules* **8**, 2774–2780.

Delaey J, **Dubruel P** and **Van Vlierberghe S** (2020) Shape-memory polymers for biomedical applications. *Advanced Functional Materials* **30**, 1909047.

Du L, **Xu ZY**, **Fan CJ**, **Xiang G**, **Yang KK** and **Wang YZ** (2018) A fascinating metallo-supramolecular polymer network with thermal/magnetic/light-responsive shape-memory effects anchored by Fe_3O_4 nanoparticles. *Macromolecules* **51**, 705–715.

Du Z, **Zhou X**, **Ye P**, **Zeng X** and **Gan CL** (2020) Shape-memory actuation in aligned zirconia nanofibers for artificial muscle applications at elevated temperatures. *ACS Applied Nano Materials* **3**, 2156–2166.

Elshazly TM, **Keilig L**, **Alkabani Y**, **Ghoneima A**, **Abuzayda M**, **Talaat S** and **Bourauel CP** (2021) Primary evaluation of shape recovery of orthodontic aligners fabricated from shape memory polymer (a typodont study). *Dentistry Journal* **9**, 31.

Essandoh M, **Dalia AA**, **Albaghdadi M**, **George B**, **Stoicea N**, **Shabsigh M** and **Rao S V** (2017) Perioperative management of dual-antiplatelet therapy in patients with new-generation drug-eluting metallic stents and bioresorbable vascular scaffolds undergoing elective noncardiac surgery. *Journal of Cardiothoracic and Vascular Anesthesia* **31**, 1857–1864.

Fan J and **Li G** (2017) High performance and tunable artificial muscle based on two-way shape memory polymer. *RSC Advances* **7**, 1127–1136.

Filion TM, **Xu J**, **Prasad ML** and **Song J** (2011) *In vivo* tissue responses to thermal-responsive shape memory polymer nanocomposites. *Biomaterials* **32**, 985–991.

Gautrot JE and **Zhu XX** (2009) Shape memory polymers based on naturally-occurring bile acids. *Macromolecules* **42**, 7324–7331.

Gong XB, **Liu LW**, **Liu YJ** and **Leng JS** (2016) An electrical-heating and self-sensing shape memory polymer composite incorporated with carbon fiber felt. *Smart Materials and Structures* **25**, 035036.

Gu SY, **Jin SP**, **Gao XF** and **Mu J** (2016) Polylactide-based polyurethane shape memory nanocomposites (Fe_3O_4/PLAUs) with fast magnetic responsiveness. *Smart Materials and Structures* **25**, 055036.

Han J, **Fei G**, **Li G** and **Xia H** (2013) High intensity focused ultrasound triggered shape memory and drug release from biodegradable polyurethane. *Macromolecular Chemistry and Physics* **214**, 1195–1203.

Hasnat Kabir M, **Hazama T**, **Watanabe Y**, **Gong J**, **Murase K**, **Sunada T** and **Furukawa H** (2014) Smart hydrogel with shape memory for biomedical applications. *Journal of the Taiwan Institute of Chemical Engineers* **45**, 3134–3138.

Hou G, **Wang F**, **Qu Z**, **Cheng Z**, **Zhang Y**, **Cai S** and **Feng X** (2018) Reversible semicrystalline polymer as actuators driven by organic solvent vapor. *Macromolecular Rapid Communications* **39**, e1700716.

Hu JL, **Meng HP**, **Li GQ** and **Ibekwe SI** (2012) A review of stimuli-responsive polymers for smart textile applications. *Smart Materials and Structures* **21**, 053001.

Inverardi N, **Scalet G**, **Melocchi A**, **Uboldi M**, **Maroni A**, **Zema L** and **Pandini S** (2021) Experimental and computational analysis of a pharmaceutical-grade shape memory polymer applied to the development of gastroretentive drug delivery systems. *Journal of the Mechanical Behavior of Biomedical Materials* **124**, 104814.

Jia H, **Gu SY** and **Chang K** (2018) 3D printed self-expandable vascular stents from biodegradable shape memory polymer. *Advances in Polymer Technology* **37**, 3222–3228.

Jing X, **Mi HY**, **Huang HX** and **Turng LS** (2016) Shape memory thermoplastic polyurethane (TPU)/poly(ε-caprolactone) (PCL) blends as self-knotting sutures. *Journal of the Mechanical Behavior of Biomedical Materials* **64**, 94–103.

Jung YC and **Cho JW** (2010) Application of shape memory polyurethane in orthodontic. *Journal of Materials Science-Materials in Medicine* **21**, 2881–2886.

Kumar B, **Hu J** and **Pan N** (2016) Smart medical stocking using memory polymer for chronic venous disorders. *Biomaterials* **75**, 174–181.

Langford T, **Mohammed A**, **Essa K**, **Elshaer A** and **Hassanin H** (2021) 4D Printing of origami structures for minimally invasive surgeries using functional scaffold. *Applied Sciences* **11**, 332.

Le Fer G and **Becker ML** (2020) 4D printing of resorbable complex shape-memory poly(propylene fumarate) star scaffolds. *ACS Applied Materials & Interfaces* **12**, 22444–22452.

Le X, **Lu W**, **Xiao H**, **Wang L**, **Ma C**, **Zhang J** and **Chen T** (2017) Fe^{3+}-, pH-, thermoresponsive supramolecular hydrogel with multishape memory effect. *ACS Applied Materials & Interfaces* **9**, 9038–9044.

Lendlein A and **Kelch S** (2002) Shape-memory polymers. *Angewandte Chemie International Edition* **41**, 2034–2057.

Lendlein A and **Langer R** (2002) Biodegradable, elastic shape-memory polymers for potential biomedical applications. *Science* **296**, 1673–1676.

Leo SY, **Zhang W**, **Zhang Y**, **Ni Y**, **Jiang H**, **Jones C** and **Taylor C** (2018) Chromogenic photonic crystal sensors enabled by multistimuli-responsive shape memory polymers. *Small* **14**, e1703515.

Li Y, **Chen H**, **Liu D**, **Wang W**, **Liu Y** and **Zhou S** (2015) pH-responsive shape memory poly(ethylene glycol)-poly(ε-caprolactone)-based polyurethane/cellulose nanocrystals nanocomposite. *ACS Applied Materials & Interfaces* **7**, 12988–12999.

Li A, **Fan J** and **Li G** (2018) Recyclable thermoset shape memory polymers with high stress and energy output via facile UV-curing. *Journal of Materials Chemistry A* **6**, 11479–11487.

Li G, **Fei G**, **Xia H**, **Han J** and **Zhao Y** (2012) Spatial and temporal control of shape memory polymers and simultaneous drug release using high intensity focused ultrasound. *Journal of Materials Chemistry* **22**, 7692.

Li G, **Gao T**, **Fan G**, **Liu Z**, **Liu Z**, **Jiang J** and **Zhao Y** (2020) Photoresponsive shape memory hydrogels for complex deformation and solvent-driven actuation. *ACS Applied Materials & Interfaces* **12**, 6407–6418.

Li X, **Lovell JF**, **Yoon J** and **Chen X** (2020) Clinical development and potential of photothermal and photodynamic therapies for cancer. *Nature Reviews Clinical Oncology* **17**, 657–674.

Li G, **Wang Y**, **Wang S**, **Liu Z**, **Liu Z** and **Jiang J** (2018) A thermo- and moisture-responsive zwitterionic shape memory polymer for novel self-healable wound dressing applications. *Macromolecular Materials and Engineering* **304**, 1800603.

Liang R, **Yu H**, **Wang L**, **Wang N** and **Amin BU** (2021) NIR light-triggered shape memory polymers based on mussel-inspired iron-catechol complexes. *Advanced Functional Materials* **31**, 2102621.

Lin C, **Zhang LJ**, **Liu YJ**, **Liu LW** and **Leng JS** (2020) 4D printing of personalized shape memory polymer vascular stents with negative Poisson's ratio structure: A preliminary study. *Science China Technological Sciences* **63**, 578–588.

Liu Y, **Lei Y**, **Hua L**, **Lu J**, **Wang K** and **Zhao C** (2021) Biomimetic self-deformation of polymer interpenetrating network with stretch-induced anisotropicity. *Chemistry of Materials* **33**, 8351–8359.

Liu YF, **Wu JL**, **Song SL**, **Xu LX**, **Chen J** and **Peng W** (2018) Thermo-mechanical properties of glass fiber reinforced shape memory polyurethane for orthodontic application. *Journal of Materials Science Materials in Medicine* **29**, 148.

Liu YF, **Wu JL**, **Zhang JX** and **Peng W** (2017) Feasible evaluation of the thermo-mechanical properties of shape memory polyurethane for orthodontic archwire. *Journal of Medical and Biological Engineering* **37**, 666–674.

Liu X, **Zhao K**, **Gong T**, **Song J**, **Bao C**, **Luo E** and **Zhou S** (2014) Delivery of growth factors using a smart porous nanocomposite scaffold to repair a mandibular bone defect. *Biomacromolecules* **15**, 1019–1030.

Lu H, **Liang F**, **Yao Y**, **Gou J** and **Hui D** (2014) Self-assembled multi-layered carbon nanofiber nanopaper for significantly improving electrical actuation of shape memory polymer nanocomposite. *Composites Part B: Engineering* **59**, 191–195.

Melocchi A, **Inverardi N**, **Uboldi M**, **Baldi F**, **Maroni A**, **Pandini S** and **Gazzaniga A** (2019) Retentive device for intravesical drug delivery based on water-induced shape memory response of poly(vinyl alcohol): Design concept and 4D printing feasibility. *International Journal of Pharmaceutics* **559**, 299–311.

Melocchi A, **Uboldi M**, **Inverardi N**, **Briatico-Vangosa F**, **Baldi F**, **Pandini S** and **Gazzaniga A** (2019) Expandable drug delivery system for gastric retention based on shape memory polymers: Development via 4D printing and extrusion. *International Journal of Pharmaceutics* **571**, 118700.

Mu S, **Zhang Y**, **Zhou J**, **Wang B** and **Wang Z** (2020) Recyclable and mechanically robust palm oil-derived epoxy resins with reconfigurable shape-memory properties. *ACS Sustainable Chemistry & Engineering* **8**, 5296–5304.

Nakasima A, **Hu JR**, **Ichinose M** and **Shimada H** (1991) Potential application of shape memory plastic as elastic material in clinical orthodontics. *European Journal of Orthodontics* **13**, 179–186.

Narayana H, **Hu J**, **Kumar B**, **Shang S**, **Ying M** and **Young RJ** (2018) Designing of advanced smart medical stocking using stress-memory polymeric filaments for pressure control and massaging. *Materials Science and Engineering: C* **91**, 263–273.

Nettleton K, **Luong D**, **Kleinfehn AP**, **Savariau L**, **Premanandan C** and **Becker ML** (2019) Molecular mass-dependent resorption and bone regeneration of 3D printed PPF scaffolds in a critical-sized rat cranial defect model. *Advanced Healthcare Materials* **8**, 1900646.

Pfau MR, **McKinzey KG**, **Roth AA**, **Graul LM**, **Maitland DJ** and **Grunlan MA** (2021) Shape memory polymer (SMP) scaffolds with improved self-fitting properties. *Journal of Materials Chemistry B* **9**, 3826–3837.

Qian C, **Zhu Y**, **Dong Y** and **Fu Y** (2017) Vapor-grown carbon nanofiber/poly(ethylene-co-vinyl acetate) composites with electrical-active two-way shape memory behavior. *Journal of Intelligent Material Systems and Structures* **28**, 2749–2756.

Razzaq MY, **Behl M**, **Kratz K** and **Lendlein A** (2013) Multifunctional hybrid nanocomposites with magnetically controlled reversible shape-memory effect. *Advanced Materials* **25**, 5730–5733.

Razzaq MY, **Behl M**, **Nöchel U** and **Lendlein A** (2014) Magnetically controlled shape-memory effects of hybrid nanocomposites from oligo(ω-pentadecalactone) and covalently integrated magnetite nanoparticles. *Polymer* **55**, 5953–5960.

Scalet G (2020) Two-way and multiple-way shape memory polymers for soft robotics: an overview. *Actuators* **9**, 10.

Senatov FS, **Niaza KV**, **Zadorozhnyy MY**, **Maksimkin AV**, **Kaloshkin SD** and **Estrin YZ** (2016) Mechanical properties and shape memory effect of 3D-printed PLA-based porous scaffolds. *Journal of the Mechanical Behavior of Biomedical Materials* **57**, 139–148.

Tamai H, **Igaki K**, **Kyo E**, **Kosuga K**, **Kawashima A**, **Matsui S** and **Uehata H** (2000) Initial and 6-month results of biodegradable poly-l-lactic acid coronary stents in humans. *Circulation* **102**, 399–404.

Tian R, **Wang Z**, **Liu J**, **Jiang Q** and **Ding B** (2021) Nucleic acid-based aggregates and their biomedical applications. *Aggregate* **2**, 133–144.

Toncheva A, **Khelifa F**, **Paint Y**, **Voue M**, **Lambert P**, **Dubois P** and **Raquez JM** (2018) Fast IR-actuated shape-memory polymers using in situ silver nanoparticle-grafted cellulose nanocrystals. *ACS Applied Materials & Interfaces* **10**, 29933–29942.

Venkatraman SS, **Tan LP**, **Joso JF**, **Boey YC** and **Wang X** (2006) Biodegradable stents with elastic memory. *Biomaterials* **27**, 1573–1578.

Wache HM, **Tartakowska DJ**, **Hentrich A** and **Wagner MH** (2003) Development of a polymer stent with shape memory effect as a drug delivery system. *Journal of Materials Science: Materials in Medicine* **14**, 109–112.

Wang K, **Amin K**, **An Z**, **Cai Z**, **Chen H**, **Chen H** and **Tang BZ** (2020) Advanced functional polymer materials. *Materials Chemistry Frontiers* **4**, 1803–1915.

Wang JG, **Gao, HC**, **Hu Y**, **Zhang NY**, **Zhou WY**, **Wang CY** and **Yang ZH** (2021) 3D printing of pickering emulsion inks to construct poly(D,L-lactide-co-trimethylene carbonate)-based porous bioactive scaffolds with shape memory effect. *Journal of Materials Science* **56**, 731–745.

Wang K, **Jia YG**, **Zhao C** and **Zhu XX** (2019) Multiple and two-way reversible shape memory polymers: Design strategies and applications. *Progress in Materials Science* **105**, 100572.

Wang K, **Jia YG** and **Zhu XX** (2015) Biocompound-based multiple shape memory polymers reinforced by photo-cross-linking. *ACS Biomaterials Science & Engineering* **1**, 855–863.

Wang K, **Jia YG** and **Zhu XX** (2017) Two-way reversible shape memory polymers made of cross-linked cocrystallizable random copolymers with tunable actuation temperatures. *Macromolecules* **50**, 8570–8579.

Wang W, **Liu D**, **Liu Y**, **Leng J** and **Bhattacharyya D** (2015) Electrical actuation properties of reduced graphene oxide paper/epoxy-based shape memory composites. *Composites Science and Technology* **106**, 20–24.

Wang L, **Razzaq MY**, **Rudolph T**, **Heuchel M**, **Nöchel U**, **Mansfeld U** and **Lendlein A** (2018) Reprogrammable, magnetically controlled polymeric nanocomposite actuators. *Materials Horizons* **5**, 861–867.

Wang K, **Si H**, **Wan Q**, **Wang Z**, **Qin A** and **Tang BZ** (2020) Luminescent two-way reversible shape memory polymers prepared by hydroxyl-yne click polymerization. *Journal of Materials Chemistry C* **8**, 16121–16128.

Wang K, **Strandman S** and **Zhu XX** (2017) A mini review: Shape memory polymers for biomedical applications. *Frontiers of Chemical Science and Engineering* **11**, 143–153.

Wang L, **Zhang FH**, **Liu YJ** and **Leng JS** (2022) Shape memory polymer fibers: materials, structures, and applications. *Advanced Fiber Materials* **4**, 5–23.

Wang K and **Zhu XX** (2018) Two-way reversible shape memory polymers containing polydopamine nanospheres: Light actuation, robotic locomotion, and artificial muscles. *ACS Biomaterials Science & Engineering* **4**, 3099–3106.

Wei Y, **Qi X**, **He S**, **Deng S**, **Liu D** and **Fu Q** (2018) Gradient polydopamine coating: A simple and general strategy toward multishape memory effects. *ACS Applied Materials & Interfaces* **10**, 32922–32934.

Wu H, **Chen R**, **Shao Y**, **Qi X**, **Yang J** and **Wang Y** (2019) Novel flexible phase change materials with mussel-inspired modification of melamine foam for simultaneous light-actuated shape memory and light-to-thermal energy storage capability. *ACS Sustainable Chemistry & Engineering* **7**, 13532–13542.

Wu G, **Panahi-Sarmad M**, **Van Vlierberghe S**, **Xu R**, **Hou X**, **Cui Z** and **Xiao X** (2022) Multi-stimuli responsive shape memory behavior of dual-switch TPU/CB/CNC hybrid nanocomposites as triggered by heat, water, ethanol, and pH. *Chemical Engineering Journal* **450**, 138253.

Xia Y, **He Y**, **Zhang F**, **Liu Y** and **Leng J** (2020) A review of shape memory polymers and composites: mechanisms, materials, and applications. *Advanced Materials* **33**, e2000713.

Xiao R, **Guo J**, **Safranski DL** and **Nguyen T** (2015) Solvent-driven temperature memory and multiple shape memory effects. *Soft Matter* **11**, 3977–3985.

Xie T (2011) Recent advances in polymer shape memory. *Polymer* **52**, 4985–5000.

Xu M, **Hua L**, **Gong L**, **Lu J**, **Wang J** and **Zhao C** (2021) Lighted up by hydrogen-bonding: Luminescence behavior and applications of AIEgen-doped interpenetrating network hydrogel. *Science China Chemistry* **64**, 1770–1777.

Xue L, **Dai S** and **Li Z** (2010) Biodegradable shape-memory block co-polymers for fast self-expandable stents. *Biomaterials* **31**, 8132–8140.

Yahara S, **Wakimoto S**, **Kanda T** and **Matsushita K** (2019) McKibben artificial muscle realizing variable contraction characteristics using helical shape-memory polymer fibers. *Sensors and Actuators A: Physical* **295**, 637–642.

Yang QX, **Fan JZ** and **Li GQ** (2016) Artificial muscles made of chiral two-way shape memory polymer fibers. *Applied Physics Letters* **109**, 183701.

Yang CS, **Wu HC**, **Sun JS**, **Hsiao HM** and **Wang TW** (2013) Thermo-induced shape-memory PEG-PCL copolymer as a dual-drug-eluting biodegradable stent. *ACS Applied Materials & Interfaces* **5**, 10985–10994.

Yu JH, **Xia H** and **Ni QQ** (2018) A three-dimensional porous hydroxyapatite nanocomposite scaffold with shape memory effect for bone tissue engineering. *Journal of Materials Science* **53**, 4734–4744.

Zeng B, **Li Y**, **Wang L**, **Zheng Y**, **Shen J** and **Guo S** (2020) Body temperature-triggered shape-memory effect via toughening sustainable poly(propylene carbonate) with thermoplastic polyurethane: toward potential application of biomedical stents. *ACS Sustainable Chemistry & Engineering* **8**, 1538–1547.

Zhang C, **Cai D**, **Liao P**, **Su JW**, **Deng H**, **Vardhanabhuti B** and **Lin J** (2021) 4D Printing of shape-memory polymeric scaffolds for adaptive biomedical implantation. *Acta Biomaterialia* **122**, 101–110.

Zhang F, **Wen N**, **Wang L**, **Bai Y** and **Leng J** (2021) Design of 4D printed shape-changing tracheal stent and remote controlling actuation. *International Journal of Smart and Nano Materials* **12**, 375–389.

Zhang H, **Xia H** and **Zhao Y** (2014) Light-controlled complex deformation and motion of shape-memory polymers using a temperature gradient. *ACS Macro Letters* **3**, 940–943.

Zhang W, **Zhang K**, **Li G**, **Yan S**, **Cui L** and **Yin J** (2018) Effects of large dimensional deformation of a porous structure on stem cell fate activated by poly(l-glutamic acid)-based shape memory scaffolds. *Biomaterials Science* **6**, 2738–2749.

Zhang FH, **Zhang ZC**, **Luo CJ**, **Lin IT**, **Liu Y**, **Leng J** and **Smoukov SK** (2015) Remote, fast actuation of programmable multiple shape memory composites by magnetic fields. *Journal of Materials Chemistry C* **3**, 11290–11293.

Zhao W, **Huang Z**, **Liu L**, **Wang W**, **Leng J** and **Liu Y** (2021) Porous bone tissue scaffold concept based on shape memory PLA/Fe_3O_4. *Composites Science and Technology* **203**, 108563.

Zhao Q, **Qi HJ** and **Xie T** (2015) Recent progress in shape memory polymer: New behavior, enabling materials, and mechanistic understanding. *Progress in Polymer Science* **49**–50, 79–120.

Zheng X, **Chen Y**, **Chen C**, **Chen Z**, **Guo Y**, **Li H** and **Liu H** (2021) High-energy-density shape memory materials with ultrahigh strain for reconfigurable artificial muscles. *Journal of Materials Chemistry B* **9**, 7371–7380.

Zhou WC, **Tan PF**, **Chen XH**, **Cen Y**, **You C**, **Tan L** and **Tian M** (2019) Berberine-incorporated shape memory fiber applied as a novel surgical suture. *Frontiers in Pharmacology* **10**, 1506.